

Novel Clinical Insights into the Pathogenesis of Posttraumatic Elbow Stiffness: An Expression Profile Analysis of Contracted Joint Capsule in Human

Nan Liu¹, Jinlei Dong¹, Lianxin Li¹, Jiajun Xu¹, Changhao Yang¹, Zhanchuan Yu², Fanxiao Liu¹

¹Department of Shandong Trauma Center, Shandong Provincial Hospital affiliated to Shandong First Medical University, Jinan, Shandong, 250014, People's Republic of China; ²Department of Shandong Trauma Center, Shandong Provincial Hospital, Cheeloo College of Medicine, Shandong University, Jinan, Shandong, 250014, People's Republic of China

Correspondence: Fanxiao Liu, Department of Shandong Trauma Center, Shandong Provincial Hospital affiliated to Shandong First Medical University, Jingshi str. 9677, Jinan, Shandong, 250014, People's Republic of China, Tel/Fax +86-0531-68773195, Email woshi631@126.com; liufanxiao@sdfmu.edu.cn

Background: Posttraumatic elbow stiffness is a complex complication with two characteristics of capsular contracture and heterotopic ossification. Currently, genomic mechanisms and pathogenesis of posttraumatic elbow stiffness remain inadequately understood. This study aims to identify differentially expressed genes (DEGs) and elucidate molecular networks of posttraumatic elbow stiffness, providing novel insights into disease mechanisms at transcriptome level.

Methods: Global transcriptome sequencing was conducted on six capsular samples from individuals with posttraumatic elbow stiffness and three control capsular samples from individuals with elbow fractures. Differentially expressed genes (DEGs), microRNAs, and long non-coding RNAs (lncRNAs) were identified and analyzed. Functional enrichment analysis was performed, and the associated protein–protein interaction (PPI) network was constructed. MicroRNAs targeting these DEGs were identified, and transcription factors (TFs) targeting DEGs were predicted using the ENCODE database. Finally, key DEGs were validated by quantitative real-time polymerase chain reaction (qRT-PCR).

Results: A total of 4909 DEGs associated with protein-coding, lncRNA and microRNA were detected, including 2124 upregulated and 2785 downregulated. Kyoto Encyclopedia of Genes and Genomes (KEGG) pathway analysis revealed that the DEGs were significantly enriched in 36 signaling pathways, notably involving inflammatory responses and extracellular matrix (ECM) receptor interactions. The protein–protein interaction (PPI) network analysis highlighted genes such as SPPI, IBSP, MMP13 and MYO1A as having higher degrees of connectivity. Key microRNAs (hsa-miR-186-5p, hsa-miR-515-5p, and hsa-miR-590-3p) and transcription factors (TFDP1 and STAT3) were predicted to be implicated in the pathogenesis of posttraumatic elbow stiffness through the microRNA-transcription factor regulatory network analysis.

Conclusion: The study provided insights into the molecular mechanisms underlying the changes in the contracted capsules associated with posttraumatic elbow stiffness. Hub genes including SPPI, IBSP, MMP13, and MYO1A, key microRNAs (hsa-miR-186-5p, hsa-miR-515-5p, hsa-miR-590-3p) and TFs (TFDP1 and STAT3) may serve as prognostic and therapeutic targets of posttraumatic elbow stiffness, and provide a new idea for the future research direction of clinical treatment.

Keywords: posttraumatic elbow stiffness, capsules, transcriptome sequencing, bioinformatic analysis, key candidate genes

Introduction

Posttraumatic elbow stiffness is a formidable complication in orthopedic practice,^{1,2} posing significant challenges to the functional mobility of the elbow joint, with the major causes of capsular contracture and heterotopic ossification,^{3–5} severely impairing the quality of life.^{6,7} Consequently, substantial efforts have been devoted to unraveling the underlying mechanisms of this pathological condition.

Prolonged joint immobilization is widely recognized as a fundamental risk factor for posttraumatic motor disability, leading to various physical and biochemical disturbances in and around the joint.⁸ These include articular cartilage erosion, reduced proteoglycan content in articular surfaces, and soft tissue contracture, particularly affecting the joint capsule.^{9–11}

Immobilization induces alterations in the composition and structure of the joint capsule, including the proliferation of connective tissues within the joint space and the formation of adhesions in the capsule and synovial membrane.^{12,13} Joint capsular fibrosis serves as a foundational aspect of posttraumatic elbow stiffness pathogenesis.¹⁴ Joint capsular fibrosis serves as a foundational aspect of posttraumatic elbow stiffness pathogenesis.¹⁵ Fibroblasts, the predominant cell type in the joint capsule, play a pivotal role in ECM synthesis and remodeling, as well as in inflammation and immune regulation.^{16,17}

Arthrofibrosis involves a complex interplay of inflammatory cytokine release, endothelial-mesenchymal transition, and growth factor signaling.¹⁸ The inflammatory response initiated after trauma can lead to contraction and adhesion of the elbow capsule due to the formation of myofibroblasts.^{19,20} Hildebrand et al reported a significant increase in the number of myofibroblasts and elevated expression of inflammatory cytokines in contracted elbow capsules.²¹ Disruption of these processes directly affects the homeostasis and organization of the joint capsule, leading to unchecked mesenchymal cell proliferation and myofibroblast formation.^{22,23}

Various signaling pathways contribute to the development of joint stiffness by regulating intracellular matrix changes, the progression of fibrosis, and a series of inflammatory reactions.^{19,24,25} The PI3K-Akt signaling pathway is pivotal in numerous cellular processes, including cell growth, migration, and differentiation. Abnormal activation of the PI3K/Akt pathway is associated with enhanced cell proliferation.²⁶ It is reported that curcumin suppressed the proliferation and migration of myofibroblasts by blocking PI3K/Akt/mTOR signaling, and thus inhibiting joint contracture.²⁷ Another study revealed that macrophage migration inhibitory factor and TGF- β 1 are other key regulators of inflammation and fibrosis of joint capsule.²⁸

Interventions targeting potential biological mechanisms underlying the disease process of arthrofibrosis have yielded limited success. Therefore, it is essential to explore the molecular mechanisms of arthrofibrosis to identify novel pharmacological therapies that could prevent, mitigate, or reverse this condition.^{14,20} Although extensive research has focused on the pathogenesis of elbow stiffness, investigations into the genomic mechanisms underlying its etiology remain limited. To date, most investigations of elbow stiffness have focused on expression of single gene or a limited number of genes.²⁹ Research on joint contracture has primarily investigated histological and molecular changes using traumatic flexion joint contracture animal models.^{30,31} Recent study characterized the gene expression profile at the early stages of the healing process of post-traumatic joint contracture using rat models.³²

In the current study, we conducted the first global transcriptomic sequencing of capsules in human undergoing surgical treatment with histologically demonstrated elbow stiffness, compared to controls without stiffness. Through global gene expression profiling, we sought to identify pathways and candidate genes implicated in the pathogenesis of this complex, clinically significant, but poorly understood disorder.

Materials and Methods

Human Tissue Collection and Processing

This study was approved by the Ethics Committee of Shandong Provincial Hospital affiliated to Shandong First Medical University. Informed consent was obtained from all patients prior to enrollment in accordance with the Declaration of Helsinki. Patients with post-traumatic elbow stiffness were continuously enrolled in the study period from August 2023 to December 2023. The control group was patients with elbow fractures during the study period. Anterior capsules were collected intraoperatively from 9 patients. At the time of surgery, the tissues were carefully excised by the operative surgeons using a scalpel to remove approximately a 2 cm x 2 cm specimen from the capsule, rinsed with phosphate buffered saline (PBS) and then immediately frozen using liquid nitrogen. After harvesting, the samples were used for whole transcriptome sequencing and qRT-PCR.

Next-Generation High-Throughput Sequencing

The quality of RNA was determined using NanoPhotometer[®] (IMPLEN, CA, USA). An mRNA library was constructed by VAHTS Universal V6 RNA-seq Library Prep Kit for Illumina[®] (NR604-01/02). Equalbit 1×dsDNA HS Assay Kit (Vazyme #EQ121), Agilent DNA 1000 Kit (Agilent, United States), and KAPA Library Quant kit (illumine, United States) universal qPCR Mix were used to assess the quality and yield of the constructed library. Finally, the mRNA was sequenced by NovaSeq 6000 (Illumina, United States).

Identification of DEGs

Based on the annotation information within the platform, probe sets were converted into their corresponding gene symbols. For genes associated with multiple probe sets, the mean expression value was calculated. The data were then normalized using quantile normalization with Illumina16 in R software (Version 3.6.2), and differentially expressed genes (DEGs) were discerned using the limma package (Version 3.42.2) within R software. Individual p-values were computed and adjusted p-values were obtained for comparative analyses using the Benjamini-Hochberg false discovery rate (FDR) correction. DEGs were selected based on criteria of $|\log_2\text{fold change (FC)}| > 2$ and $p\text{-value} < 0.05$. Heatmaps and volcano plots depicting the DEGs were generated utilizing the ggplot2 package in R software.³³

Functional and Pathway Enrichment Analyses of DEGs

The up- and downregulated DEGs were uploaded to the Database for Annotation, Visualization, and Integrated Discovery (DAVID) version 6.8 Beta (<https://david-d.ncifcrf.gov/>),³⁴ and further analyzed using gene ontology (GO) and Kyoto Encyclopedia of Gene and Genome (KEGG) analysis in the R ggplot2 package. The significance criterion was set at $p\text{-value} < 0.05$.

Protein-Protein Interaction Network Construction and Module Analysis

The protein-protein interaction (PPI) network of DEGs was predicted using the multiple protein online tool within the STRING database (version 11.0, <http://string-db.org>), a widely recognized platform for retrieving interacting genes,³⁵ and visualized in Cytoscape software (Version 3.6.2).^{36–38} The most significant modules within the PPI network were identified and illustrated using Molecular Complex Detection (MCODE), an analytical tool in Cytoscape designed for detecting densely interconnected regions in complex networks. Selection criteria encompassed MCODE scores > 5 , node score cutoff = 0.2, degree cutoff = 2, max depth = 100, and k-score = 2. Following the identification of key modules, a biological process analysis of the top 20 genes was conducted and visualized using the Biological Networks Gene Ontology (BiNGO) plugin (version 3.0.3) in Cytoscape.³⁹

Hub Gene Selection

The top 10 hub genes within the PPI network were identified using Maximal Clique Centrality (MCC), Degree, and Maximum Neighborhood Component (MNC) algorithms, as implemented in the cytoHubba plugin in Cytoscape.^{40,41}

TF-DEG Network and miRNA-DEG

Network construction involved predicting transcription factors (TFs) targeting DEGs using the ENCODE database within Network Analyst (<https://www.networkanalyst.ca/faces/home.xhtml>), a widely recognized visual analytics platform for comprehensive gene expression profiling and meta-analysis. Concurrently, microRNA-DEG interactions were identified through the TarBase, miRTarBase, and miRecords databases. The resulting TF-DEGs and miRNA-DEGs interaction pairs were retained for subsequent analysis.

TF-miRNA Integrated Network Construction

The integrated network of TF-miRNA was constructed according to the TF-DEG and miRNA-DEG networks. The coregulated DEGs targeted by miRNAs and TFs were identified and prioritized. Following this selection, the associated

miRNAs and TFs were extracted. Eventually, the integrated regulatory network was constructed and visualized in Cytoscape software (Version 3.6.2).³³

Quantitative Real-Time Reverse Transcription Polymerase Chain Reaction (qRT-PCR)

Key DEGs including MMP13, IBSP, LBS, RRM2, CHI3L1, GRIA1, ECRG4, MYO1A, SPP1 and TNXB were chosen for qRT-PCR assay on the RNA of stiff capsule and control group. Purified DNA-free RNA samples were extracted from capsule tissues using the RNeasy Mini Kit, reverse transcribed using a One Step PrimeScript[®] miRNA cDNA Synthesis Kit (Takara, Japan, D350A) and amplified using SYBR[®] Premix Ex TaqTM II kit (Takara, Japan, DRR820A) according to the manufacturer's instructions. Gene expression of each target was calculated using the $\Delta\Delta CT$ method after normalization to the expression of GAPDH housekeeping genes.

Statistical Analysis

GraphPad Prism Software version 8.1.0 (GraphPad Software Inc., USA) was performed to statistical analyses and creates graphs. One-way analysis of variance (ANOVA) was used to compare the gene expression and levels of inflammatory factors. The results are presented as the means \pm standard errors (SEM), and a p-value < 0.05 was considered statistically significant.

Results

Clinical Characteristics of Patients

Capsules of human stiff elbows were obtained from 6 patients, two males and four females, with a mean age of 42 years \pm 12 years (range, 31–61 years) at the time of contracture release and an average 7.7 \pm 3.8 months (range, 2–13 months) after injury. The original injuries all were intraarticular fractures: two patients had elbow fractures, one patient had a radial head fracture, one patient had an olecranon fracture, one patient had an ulnar styloid fracture, one patient had proximal radius and ulna fractures. Control capsules were obtained from three patients with elbow fractures (47 \pm 16 years old; one male and two females) that were free of contractures. There were no significant differences comparing the average age and the gender distribution of the patient and control groups. The basic information of the included patients was presented in Table 1.

Data Normalization

To assess data normalization and cross-comparability, box plots and principal component analysis (PCA) were used to confirm biological variability among samples. Figure S1 shows that after normalization, the black lines are nearly aligned, indicating strong standardization, which enhances the reliability of further analyses. Additionally, Figure S2 illustrates the distinct clustering of control patients and those with stiff elbows, reflecting their unique gene expression profiles and supporting the validity of our research.

Table 1 The Basic Information of the Included Patients

Group	No.	Sex	Age (years)	Time from stiffness to surgery (months)	Initial fracture type	Side	Ulnar nerve symptoms	BMI	Past Medical History
Elbow stiffness	T_1	female	58	11	elbow fracture	right	yes	20.5	no
	T_2	male	33	4	elbow fracture	left	no	17.7	no
	T_3	female	33	13	olecranon fracture	left	no	35.8	no
	T_4	male	35	2	ulnar styloid fracture	right	no	26.8	no
	T_5	female	31	7	radial head fracture	right	yes	18.6	no
	T_6	male	61	9	proximal radius and ulna fractures	right	yes	22.9	no
No-elbow stiffness	C_1	female	69	N/A	distal humeral fracture	right	no	21.1	uterine fibroids
	C_2	male	44	N/A	terrible triad	left	no	26.1	no
	C_3	female	29	N/A	radial head fracture	left	no	25.4	no

Note: N/A, no available.

Identification of DEGs

The high-throughput sequencing data from the capsule tissues were subsequently analyzed to identify DEGs based on predefined criteria. In total, 4909 DEGs were detected between the stiff elbow group and the control group, including 3492 associated with protein-coding, 1343 associated with LncRNA and 74 associated with microRNA (Figure 1A). According to the adjusted p -value < 0.05 , there were 2124 upregulated (1483 Protein-coding, 603 LncRNA and 38 MicroRNA) and 2785 downregulated (2009 Protein-coding, 740 LncRNA and 36 MicroRNA) DEGs (Figure 1B). The top ten up- and down-regulated protein-coding DEGs, LncRNAs, and MicroRNAs were presented in Figure 1D–F. The top five upregulated protein-coding DEGs were SLN, HLF, IGLL5, SCNN1B and ALKAL2, and the top five down-regulated were MMP13, IBSP, LBP, AMTN and CHI3L1. The top five upregulated LncRNAs were ENSG00000255021, ENSG00000286289, ENSG00000269124, LINC01819 and ENSG00000229969, and the top five downregulated LncRNAs were ENSG00000230699, ENSG00000285846, LINC01614, MGC27382 and APOBEC3B-AS1. The top five upregulated MicroRNAs were has-miR-6717, has-miR-7152, has-miR-3650, has-miR-143 and has-miR-4697, and the top five downregulated MicroRNAs were has-hsa-miR-4497, hsa-miR-3917, hsa-miR-147B, hsa-miR-621 and hsa-miR-635. In addition, a volcano plot of all DEGs was generated using the R ggplot2 package (Figure 2A–C). Expression profiles of top 50 significant DEGs in each sample were identified and shown as heatmap (Figure 2D–F).

Functional Enrichment Analysis of DEGs

GO and KEGG pathway enrichment analysis of DEGs was performed to identify the most relevant biological processes (BPs), molecular functions (MFs), cellular components (CCs), and pathways. The top 5 enriched terms in BP, CC, MF of capsules in stiff elbows were presented in Figure 3A. KEGG pathway enrichment analysis revealed that the DEGs of the stiff elbow group were enriched in the inflammatory response, extracellular matrix, ECM-receptor interaction, PI3K-AKT signaling pathway, cell proliferation, apoptotic process, angiogenesis, wound healing. Some

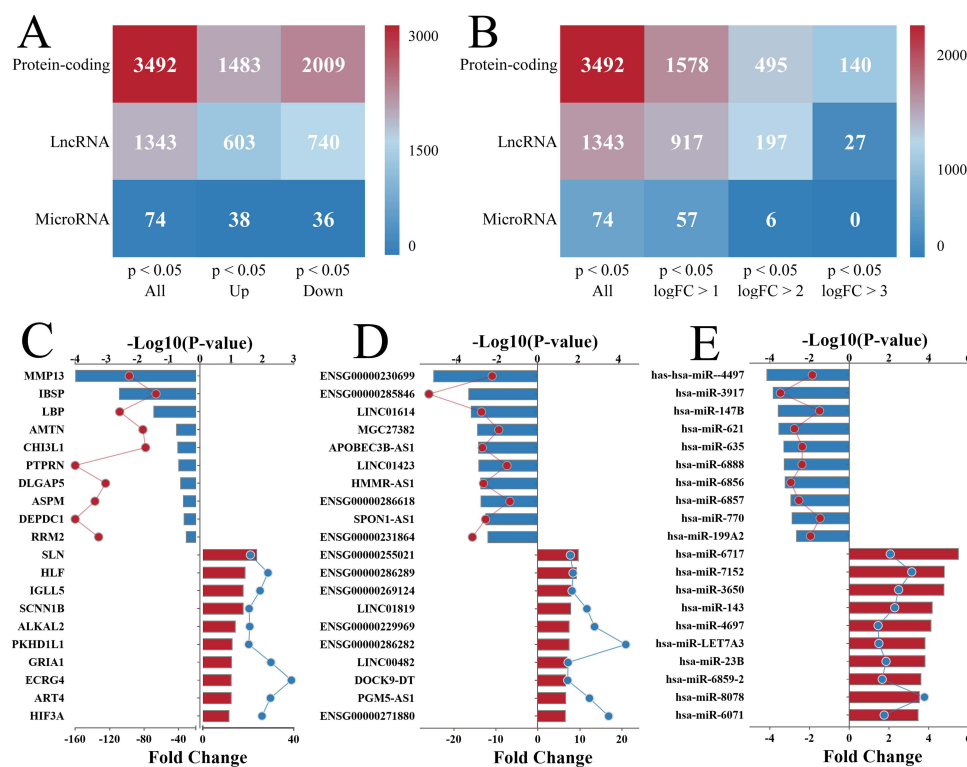


Figure 1 Differentially expressed genes (DEGs) within the posttraumatic contracted capsules. (A) The values represent the number of DEGs (according to the adjusted p -value < 0.05) of protein-coding genes, and lncRNA-coding genes and microRNA-coding genes; (B) The number of DEGs according to the adjusted p -value < 0.05 and different criteria of logFC; (C–E) The top ten up- and down-regulated protein-coding DEGs (C), LncRNAs (D), and MicroRNAs (E). Red indicates relatively up-regulated, and blue indicates relatively down-regulated.

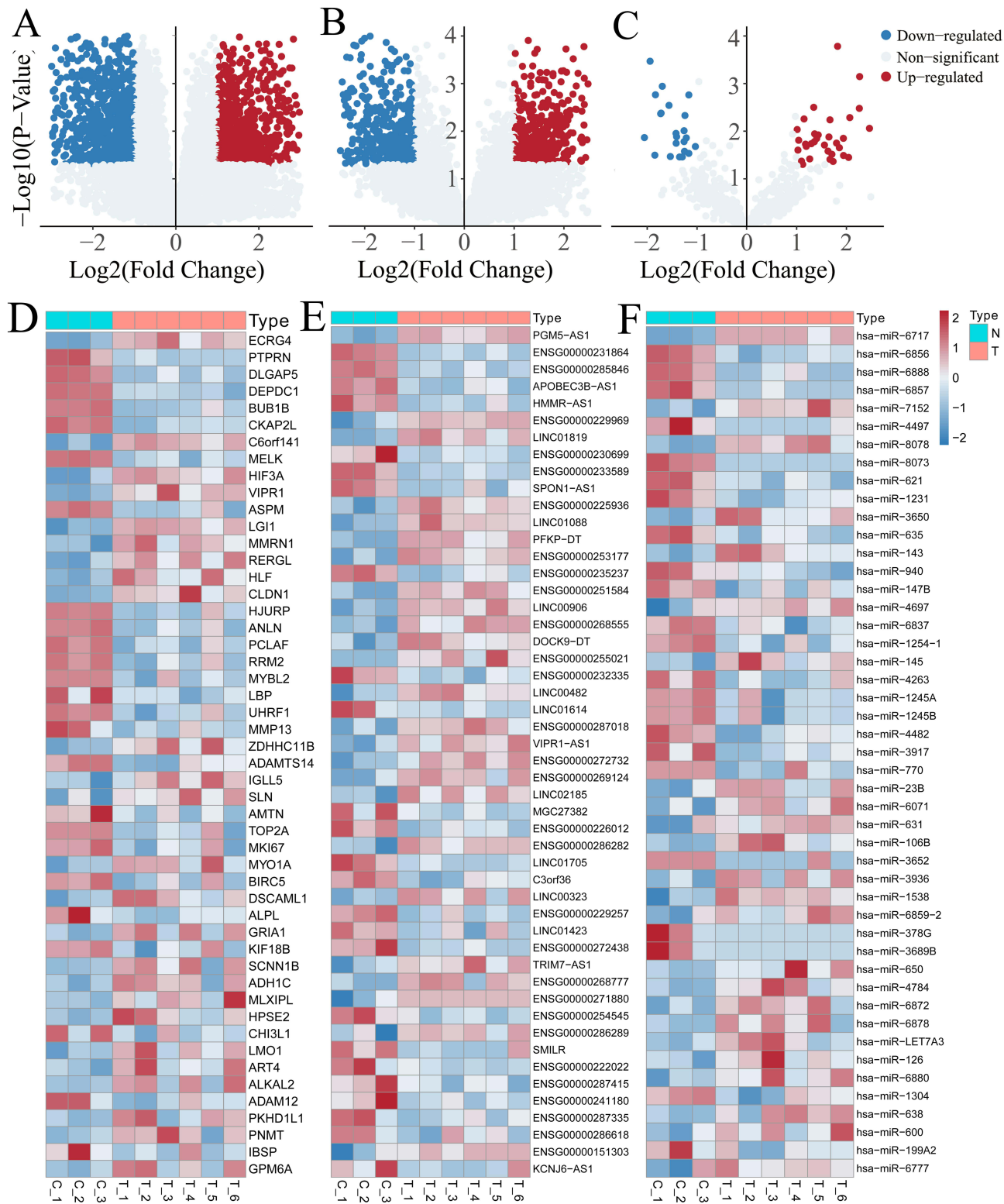


Figure 2 DEGs associated with Protein-coding (A), lncRNAs (B), and microRNAs (C) were shown with DEGs. The heatmap showed the expression profiles of top 50 significant DEGs of Protein-coding (D), lncRNA-coding genes (E), microRNA-coding genes (F). A Red indicates relatively up-regulated, and blue indicates relatively down-regulated. DEGs were identified by the criteria of $|\log_2\text{fold change (FC)}| > 2$ and adj. p. val < 0.05 . Abbreviations: DEGs, differentially expressed genes.

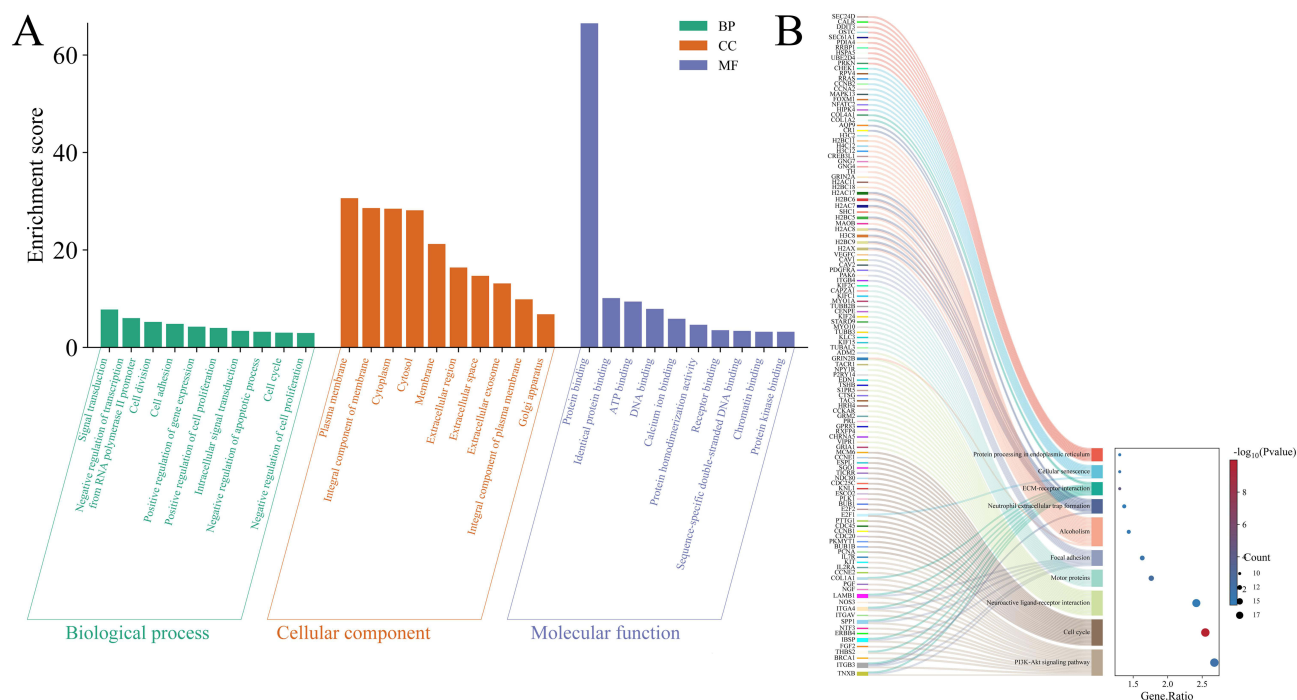


Figure 3 (A) GO enrichment in relevant biological processes, molecular functions, cellular components. **(B)** KEGG pathways of targets of the DEGs. Abbreviations: DEGs, differentially expressed genes; GO, Gene Ontology; KEGG, Kyoto Encyclopedia of Genes and Genomes.

DEGs associated with fibrosis and osteogenesis were enriched in PI3K-AKT signaling pathway, such as IBSP, SPP1 and TNXB (Figure 3B).

PPI Network Construction and Module Analysis

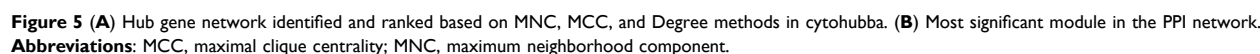
The interactions between the proteins expressed from DEGs, which consisted of 140 nodes and 2209 edges (Figure 4), were constructed from the STRING database and visualized using Cytoscape. Two significant modules (Figure 5B) were obtained by module analysis in the PPI network using MCODE from Cytoscape based on the aforementioned criteria. In addition, 5 of the top genes with relatively high connectivity degrees (≥ 20) were BUB1, TOP2A, BUB1B, MKI67, KIF11, and AURKB. The crucial nodes with a high MCODE score in this module were ALPL, MMP13, SPP1 and IBSP, which are associated with arthritis and osteophyte formation, and have potential role in the occurrence of elbow stiff. The biological process analysis of the top 20 genes was performed and visualized using BiNGO in Cytoscape, which is shown in Figure S3.

Hub Gene Selection

Hub genes were selected by CytoHubba. The top 20 hub genes, which were selected based on the 3 most commonly used classification methods in CytoHubba, are presented in Table 2. By overlapping the first 20 genes, 16 central genes (KIF20A, BUB1B, KIF11, MKI67, BUB1, CEP55, AURKB, PBK, TOP2A, CENPF, TTK, MELK, CDCA8, KIF2C, BIRC5, and ASPM) were consequently identified as presented in Figure 5A.

Construction of the TF-DEG Network Analysis

According to TF binding site data and genetic coordinate position information provided in ENCODE, a potential regulatory network between DEGs and TFs was constructed to analyze the functional roles of selected DEGs. A total of 40 associations between 16 TFs and 14 DEGs were predicted. As shown, the upregulated gene HLF might be associated with 4 TFs (FOXA3, TFDPI, BCL6 and EZH2), and downregulated gene RRM2 might have interaction with 10 TFs (TFDPI, BCL6, KLF9, NRF1, ZNF644, ZNF324, SIN3A, CTCF and PML) (Figure 6A).



The microRNA-DEG pairs were identified through network analysis of 20 DEGs using the TarBase, miRTarBase and miRecords databases. Ultimately, a total of 26 associations between 11 microRNAs and 8 DEGs were identified, and then the network was visualized in Cytoscape. The downregulated gene RRM2 regulated 5 interacting microRNAs, including

Table 2 List of the Top 20 hub Genes Selected by MCC, MNC and Degree Methods in cytoHubb

Degree	MCC	MNC
BUB1	BUB1	KIF20A
TOP2A	TOP2A	CEP55
BUB1B	BUB1B	BUB1
MKI67	KIF11	ASPM
KIF11	AURKB	NUF2
AURKB	CENPF	TOP2A
CENPF	BIRC5	AURKB
BIRC5	CDC20	CENPF
CDC20	KIF20A	MELK
KIF20A	CEP55	KIF2C
CEP55	ASPM	PBK
ASPM	KIF2C	BUB1B
KIF2C	CDCA8	CDCA8
CDCA8	MKI67	NEK2
TTK	TTK	RRM2
CCNB1	DLGAP5	BIRC5
DLGAP5	TPX2	MKI67
TPX2	MELK	TTK
MELK	PBK	CDC45
PBK	NEK2	KIF11

Abbreviations: MCC, maximal clique centrality; MNC, maximum neighborhood component.

hsa-mir-186-5p, hsa-let-7a-5p, hsa-mir-17-5p, hsa-mir-2276-5p, hsa-mir-4672. A hub microRNA, hsa-mir-186-5p, was predicted to interact with 3 DEGs, including RRM2, DLGAP5, and DEPDC1 (Figure 6B).

TF-miRNA Interaction Network

The TF-microRNA interaction network was constructed through network analysis of top 20 DEGs (10 up, 10 down) in Cytoscape including 12 DEGs, 15 TFs, and 14 microRNAs, with 34 associations between the TFs and DEGs and 35 associations between the miRNAs and DEGs. We separately analyzed the degree of 12 DEGs in the TF-DEG network and the microRNA-DEG network (Table 3). We found that the upregulated gene HLF might be regulated by 6 TFs (SP1, RORA, FOSL1, MYC, NFYA and ZEB1) and associated with 4 microRNAs (has-miR-96, hsa-miR-103, hsa-miR-590-3p and hsa-miR-137). The downregulated gene CHI3L1 might be regulated by 5 TFs (SP1, FOSL1, ATF2, JUN, USF1 and SPI1), and had interaction with 2 microRNAs (hsa-miR-296-3p and hsa-miR-623) (Figure 7).

Gene Expressions Validation by qRT-PCR Analysis

To validate the gene expressions, qRT-PCR analysis was performed. The results confirmed a significant increase in the relative mRNA expression levels of MMP13, IBSP, LBS, RRM2, CHI3L1, GRIA1, ECRG4, MYO1A, SPP1 and TNXB in the stiff elbow capsule compared to the control group (Figure 8). Notably, the results of the gene expression examined by qRT-PCR and high-throughput sequencing were highly correlated.

Discussion

Elbow stiffness is a common complication of elbow trauma that causes movement disorders and functional loss, significantly affecting the quality of life.⁴² The primary cause of elbow stiffness is the contraction of soft tissues

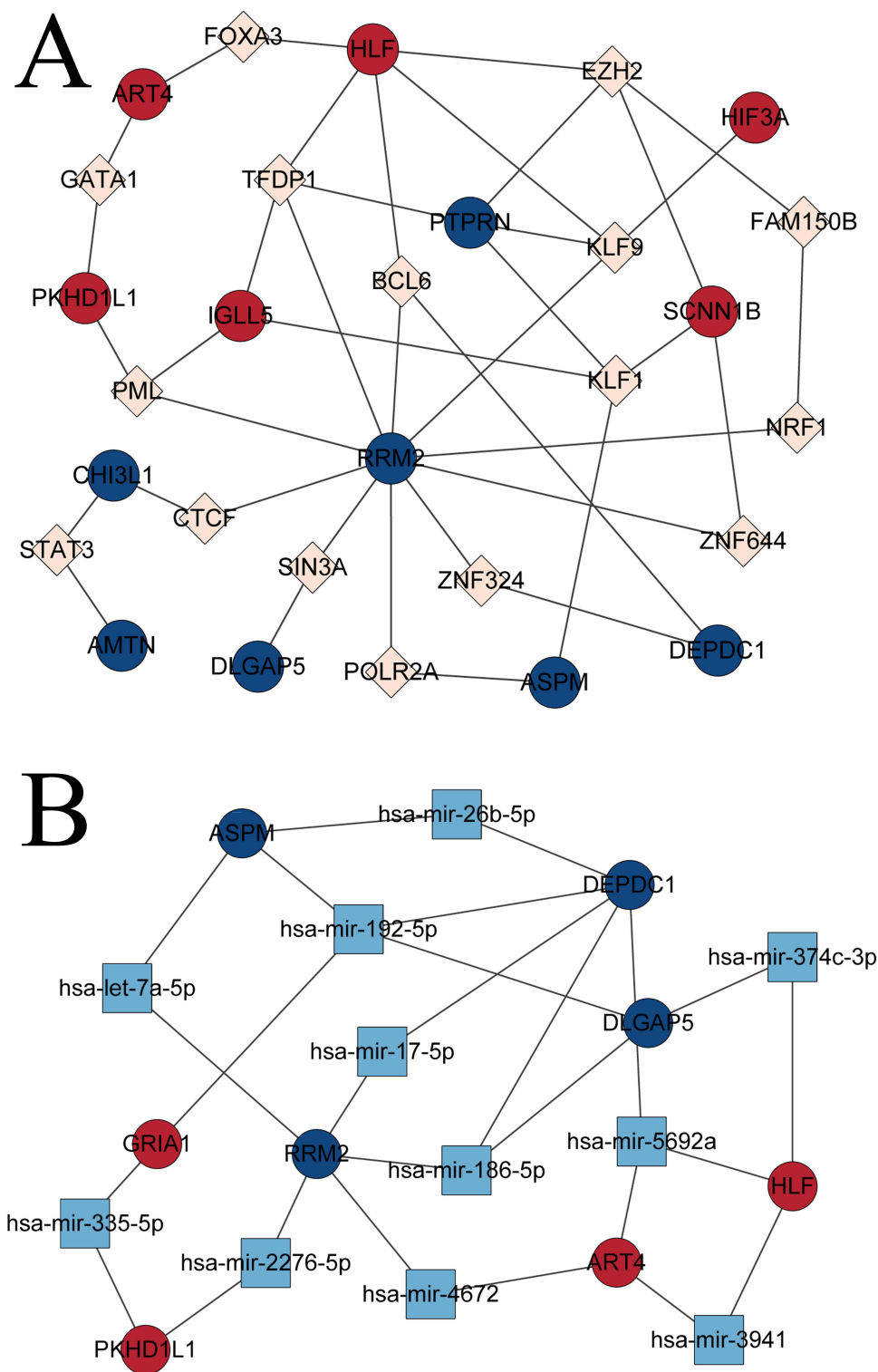


Figure 6 (A) The network of TF-DEG was obtained from the ENCODE database. (B) The network of DEG-miRNA was obtained from the tarbase, miRTarBase, and miRecords databases. The circles indicates DEGs (red indicates upregulated genes, and blue indicates the downregulated genes), the diamonds indicates TFs, and the squares indicates miRNAs.

Abbreviations: ENCODE, Encyclopedia of DNA Elements; TF, transcription factor; DEG, differentially expressed gene; miRNA, microRNA.

Table 3 Co-DEGs Regulated by TF and miRNAs

TF	DEGs	Gene counts
MAX	FAM150B, RRM2, DEPDC1, HIF3A	4
ATF2	FAM150B, CHI3LI	3
JUN	RRM2, CHI3LI, PTPRN	3
MYC	RRM2, HIF3A, HLF	3
FOSL1	CHI3LI, HLF	2
RORA	GRIA1, HLF	2
NFYA	DLGAP5, RRM2	2
SREBF2	AMTN, DEPDC1	2
USF1	CHI3LI, DEPDC1, HIF3A	3
ZEB1	SLN, HIF3A	2
SPI	HIF3A, HLF	2
SPII	PKHD1LI, CHI3LI	2
REST	RRM2, PTPRN	2
GATA1	PKHD1LI, SLN	2
miRNA	DEGs	Gene counts
hsa-miR-608	SCNN1B, GRIA1, HIF3A	3
hsa-miR-590-3p	PKHD1LI, DEPDC1, SLN	3
hsa-miR-296	CHI3LI, SLN, HIF3A	3
hsa-miR-623	DLGAP5, CHI3LI	2
hsa-miR-617	DLGAP5, SLN	2
hsa-miR-522	CHI3LI, GRIA1	2
hsa-miR-25	FAM150B, GRIA1	2
hsa-miR-96	DEPDC1, GRIA1	2
hsa-miR-515	DLGAP5, HIF3A	2
hsa-miR-485	PTPRN, HIF3A	2
hsa-miR-137	PKHD1LI, GRIA1	2
hsa-miR-124	FAM150B, DEPDC1	2
hsa-miR-103	AMTN, SLN	2
hsa-let-7a	AMTN, HIF3A	2

Abbreviations: DEGs, differentially expressed genes; miRNAs, microRNAs.

following the initial injury, which is exacerbated by prolonged immobilization.⁴³ Despite extensive efforts to understand and prevent elbow joint contracture, its exact etiology remains unclear.^{44,45}

Our team identified global transcriptomic differences between normal and pathological tissues in patients with elbow stiffness by using RNA sequencing. This method allowed us to screen for DEGs, revealing specific genes and biological pathways involved in the development of elbow stiffness. Understanding these mechanisms will enable more accurate diagnosis and classification of posttraumatic elbow stiffness and assist in developing targeted prevention strategies.

The informatics analysis of gene profiles in stiff and control elbow capsules identified 4909 DEGs, including 3492 associated with protein-coding, 1343 associated with lncRNA and 74 associated with microRNA. This discovery enhances our understanding of the regulatory factors contributing to elbow stiffness.

The most significantly downregulated gene was MMP13, which encodes a key enzyme responsible for the degradation of ECM components.⁴⁶ Polymorphisms in MMP genes have been linked to various orthopedic conditions, including posterior tibial tendinopathy, rotator cuff tears, post-repair stiffness, and Dupuytren's disease.⁴⁷ MMPs primarily degrade ECM components, including collagen, laminin, fibronectin, and proteoglycans. ECM homeostasis is maintained by balancing collagen deposition and removal. An imbalance in this process can lead to pathology: excessive collagen removal may result in tendinous ruptures, such as posterior tibial tendon and rotator cuff tears, while excessive deposition can lead to fibrotic conditions like Dupuytren's disease and adhesive capsulitis.^{47,48} MMP13 is the main enzyme

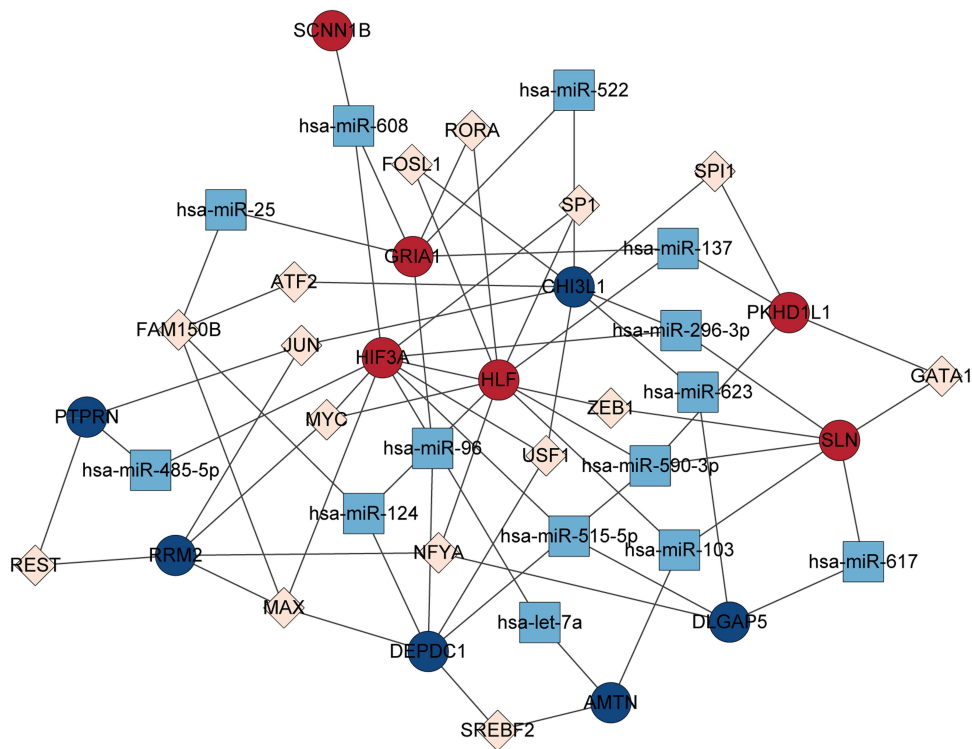


Figure 7 Integrative regulatory network of TF-DEG-miRNA. The circles indicates DEGs (red indicates upregulated genes, and blue indicates the downregulated genes), the diamonds indicates TFs, and the squares indicates miRNAs.
Abbreviations: TF, transcription factor; DEG, differentially expressed gene; miRNA, microRNA.

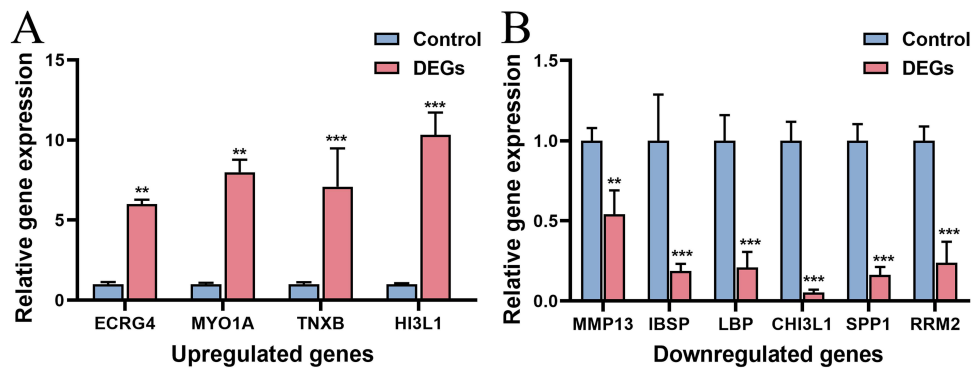


Figure 8 qRT-PCR Analysis of the expression levels of 10 important DEGs in contracted capsules of posttraumatic elbow stiffness and control samples. **(A)** qRT-PCR Analysis of the expression levels of up-regulated DEGs. **(B)** qRT-PCR Analysis of the expression levels of down-regulated DEGs. **P < 0.001, ***P < 0.001, compared with control samples.

responsible for collagen fiber degradation.⁴⁶ Its downregulation in contracted elbow capsules indicates a potential role in the development of elbow stiffness.

The GO and KEGG pathway enrichment analysis revealed that the DEGs in the stiff elbow group are involved in several critical biological processes and pathways. These include the inflammatory response, extracellular matrix organization, ECM-receptor interaction, cell proliferation, apoptosis, angiogenesis, and wound healing. Notably, the DEGs are predominantly associated with the PI3K-Akt signaling pathway, which plays a key role in the proliferation and migration of myofibroblasts, such as TNXB, IBSP, SPP1, COL1A1, COL1A2, COL4A2, COL4A1, PPP2R2B, IL2RA, COL6A1, KIT, IL2RB, COL6A3, COL6A5, and IL7R.

The PI3K/Akt signaling pathway plays an important role in many cellular processes, including cell growth, migration, and differentiation. Studies indicated that it is also crucial in the development of joint contracture.^{49,50} In fibrotic joints, activation of the PI3K-Akt pathway promotes the proliferation of myofibroblasts.⁴⁹ IBSP (integrin-binding sialoprotein), also known as bone sialoprotein II, was found to be downregulated in post-traumatic capsules. IBSP is highly expressed in osteoblasts, osteoclasts, and hypertrophic chondrocytes and is involved in bone matrix mineralization and turnover, as well as in regulating cell adhesion, proliferation, and differentiation.^{51,52} Downregulation of IBSP can activate the PI3K/Akt pathway, leading to increased transcription of osteoblast-specific target genes.⁵³ SPP1 (osteopontin) is a highly phosphorylated glycoprotein that was found to be downregulated in contracted elbow capsules and is associated with the PI3K-Akt signaling pathway.⁵⁴ As a key non-collagenous protein, SPP1 plays crucial roles in regulating bone cell adhesion, osteoclast function, and matrix mineralization, and it is closely linked to the development of various bone diseases.⁵⁵ Studies have shown that miR-186-5p inhibits chondrocyte apoptosis in osteoarthritis (OA) by interacting with SPP1 and modulating the PI3K-Akt pathway.⁵⁶ In our research, SPP1 was downregulated and miR-186-5p was predicted as a key microRNA in the contracted capsules, suggesting a potential in pathogenesis of posttraumatic elbow stiffness.

TFs and microRNAs have emerged as key regulatory elements in the pathogenesis of elbow stiffness. To elucidate potential interactions among TFs, DEGs, and microRNAs in stiff capsules, we constructed a TF-microRNA interaction regulatory network. Within this network, TFDP1 was observed to regulate four DEGs (HLF, IGLL5, RRM2, and PTPRN), KLF9 exhibited regulation over four DEGs (HIF3A, HLF, RRM2, and PTPRN), and KLF1 exerted regulatory control over four DEGs (SCNN1B, IGLL5, PTPRN, and ASPM). TFDP1 is a crucial transcription factor that facilitates the transcription of genes targeted by E2F, thereby modulating cell differentiation and the cell cycle by interacting with E2F proteins.⁵⁷ TFDP1 mRNA levels are differentially expressed in primary chondrocytes depending on osteoarthritis (OA) severity.⁵⁸ TFDP1 also interacts with pRB and p53 to regulate the cell cycle and apoptosis.⁵⁹ The downregulated gene CHI3L1 might be regulated by 5 TFs and had interaction with 2 microRNAs. CHI3L1 plays a crucial role in preventing inflammation as well as in tissue repair and remodeling by regulating a variety of fundamental biological processes, including apoptosis, inflammasome activation, macrophage differentiation, ECM regulation, and parenchymal scar formation,⁶⁰ which are also associated with fibrosis and joint contracture.

Multiple studies have shown that miRNAs play a key role in maintaining bone homeostasis and the development of bone diseases.^{61–65} Thus, we constructed a DEG-miRNA regulatory network to show the potential interactions among identified DEGs and RNAs during capsular contracture. In the networks, hsa-miR-186-5p may play an important role because it connects with three key genes, which was also confirmed to be associated with numerous physiological processes, including migration, invasion, proliferation and inflammation, as well as the development of OA,^{62,66} but currently, there is no direct evidence to prove the role of this miRNA for the development of posttraumatic elbow stiffness.

For the first time, the global transcriptome of post-traumatic elbow capsules has been systematically detected and analyzed. This study provides new directions and molecular targets for further investigation into post-traumatic elbow stiffness through high-throughput sequencing and rigorous bioinformatics analysis. We identified several key genes, transcription factors, and miRNAs that may play crucial roles in this condition. However, it must be acknowledged that this is foundational research. Although multiple hub genes, key miRNAs, and transcription factors were identified, their detailed functions in posttraumatic elbow stiffness need to be further elucidated through *in vivo* and *in vitro* studies. The small sample size in the study might lead to insufficient accuracy of the results, and we will continue to increase histological and cytological validation of clinical samples in the future.

Conclusion

This study represents the first comprehensive global transcriptome sequencing of human post-traumatic elbow capsules, identifying hub genes, functional terms, and predicted target genes that contribute to understanding the molecular mechanisms underlying post-traumatic elbow stiffness. Key hub genes such as SPP1, IBSP, MMP13, and MYO1A appear to play significant roles in capsular fibrosis. Additionally, hsa-miR-186-5p has emerged as a potential regulator of chondrocyte proliferation and inflammation. Our findings enhance the understanding of capsular contraction mechanisms and offer theoretical support for the clinical treatment of post-traumatic elbow stiffness. Understanding the pathogenesis of elbow stiffness after trauma has guiding significance for clinical treatment, such as screening drugs for genetic

intervention. The regulatory pathways involved in these genes have guiding significance for disease prevention and provide future research directions.

Data Sharing Statement

The datasets used and/or analyzed during the current study are available from the corresponding author on reasonable request.

Institutional Review Board Statement

All studies were approved by the Ethics Committee of Shandong Provincial Hospital affiliated to Shandong First Medical University (SWYX: NO. 2022-590).

Informed Consent Statement

Written informed consent was obtained from each participant prior to inclusion in the study.

Consent for Publication

Not applicable.

Author Contributions

All authors made a significant contribution to the work reported, whether that is in the conception, study design, execution, acquisition of data, analysis and interpretation, or in all these areas; took part in drafting, revising or critically reviewing the article; gave final approval of the version to be published; have agreed on the journal to which the article has been submitted; and agree to be accountable for all aspects of the work.

Funding

This work was partially supported by the Natural Science Foundation of Shandong Province (No. ZR2021QH307; No. ZR2023QH498; No. ZR2021MH013; No. ZR2022MH056), the Shandong Province Major Scientific and Technical Innovation Project (No. 2021SFGC0502), and the Jinan Clinical Medical Science and Technology Innovation Plan (NO. 202328065). The authors, their immediate families, and any research foundations with which they are affiliated have not received any financial payments or other benefits from any commercial entity related to the subject of this article.

Disclosure

The authors declare no competing interests.

References

1. Zhang D, Nazarian A, Rodriguez EK. Post-traumatic elbow stiffness: pathogenesis and current treatments. *Shoulder Elbow*. 2020;12(1):38–45. doi:10.1177/1758573218793903
2. Myden C, Hildebrand K. Elbow joint contracture after traumatic injury. *J Shoulder Elbow Surg*. 2011;20(1):39–44. doi:10.1016/j.jse.2010.07.013
3. Sun Z, Liu H, Hu Y, et al. KLF2 / PPAR γ axis contributes to trauma-induced heterotopic ossification by regulating mitochondrial dysfunction. *Cell Prolif*. 2024;57(1):e13521. doi:10.1111/cpr.13521
4. Lindenhovius AL, Jupiter JB. The posttraumatic stiff elbow: a review of the literature. *J Hand Surg Am*. 2007;32(10):1605–1623. doi:10.1016/j.jhsa.2007.09.015
5. Wahl EP, Lampley AJ, Chen A, et al. Inflammatory cytokines and matrix metalloproteinases in the synovial fluid after intra-articular elbow fracture. *J Shoulder Elbow Surg*. 2020;29(4):736–742. doi:10.1016/j.jse.2019.09.024
6. Hildebrand KA. Posttraumatic elbow joint contractures: defining pathologic capsular mechanisms and potential future treatment paradigms. *J Hand Surg Am*. 2013;38(11):2227–2233. doi:10.1016/j.jhsa.2013.07.031
7. Guglielmetti CLB, Gracitelli MEC, Assunção JH, et al. Randomized trial for the treatment of post-traumatic elbow stiffness: surgical release vs. rehabilitation. *J Shoulder Elbow Surg*. 2020;29(8):1522–1529. doi:10.1016/j.jse.2020.03.023
8. Xu J, Yu Z, Liu F, Lu S, Li L. Is anterior transposition of the ulnar nerve necessary for post-traumatic elbow stiffness? A retrospective study. *J Orthop Surg Res*. 2024;19(1):720. doi:10.1186/s13018-024-05220-x
9. Hildebrand KA, Zhang M, Hart DA. High rate of joint capsule matrix turnover in chronic human elbow contractures. *Clin Orthop Relat Res*. 2005;439:228–234. doi:10.1097/01.blo.0000177718.78028.5c

10. Born CT, Gil JA, Goodman AD. Joint contractures resulting from prolonged immobilization: etiology, prevention, and management. *J Am Acad Orthop Surg*. 2017;25(2):110–116. doi:10.5435/JAAOS-D-15-00697
11. Dai J, Zhang G, Li S, Xu J, Lu J. Arthroscopic treatment of posttraumatic elbow stiffness due to soft tissue problems. *Orthop Surg*. 2020;12(5):1464–1470. doi:10.1111/os.12787
12. Gonzalez-Alvarez ME, Sanchez-Romero EA, Turroni S, Fernandez-Carnero J, Villafane JH. Correlation between the altered gut microbiome and lifestyle interventions in chronic widespread pain patients: a systematic review. *Medicina (Kaunas)*. 2023;59. doi:10.3390/medicina59020256.
13. Martinez-Pozas O, Sánchez-Romero EA, Beltran-Alacreu H, et al. Effects of orthopedic manual therapy on pain sensitization in patients with chronic musculoskeletal pain: an umbrella review with meta-meta-analysis. *Am J Phys Med Rehabil*. 2023;102(10):879–885. doi:10.1097/PHM.0000000000002239
14. Li F, Fan C, Zeng B, et al. Celecoxib suppresses fibroblast proliferation and collagen expression by inhibiting ERK1/2 and SMAD2/3 phosphorylation. *Mol Med Rep*. 2012;5(3):827–831. doi:10.3892/mmr.2011.722
15. Zhou Y, Zhang QB, Zhong HZ, et al. Rabbit model of extending knee joint contracture: progression of joint motion restriction and subsequent joint capsule changes after immobilization. *J Knee Surg*. 2020;33(01):15–21. doi:10.1055/s-0038-1676502
16. Zhang Y, Liu Z, Wang K, et al. Macrophage migration inhibitory factor regulates joint capsule fibrosis by promoting TGF-beta1 production in fibroblasts. *Int J Biol Sci*. 2021;17(7):1837–1850. doi:10.7150/ijbs.57025
17. Moldovan F. Correlation between peripheric blood markers and surgical invasiveness during humeral shaft fracture osteosynthesis in young and middle-aged patients. *Diagnostics (Basel)*. 2024;14(11). doi:10.3390/diagnostics14111112
18. Zhang QB, Huo L, Li M, et al. Role of hypoxia-mediated pyroptosis in the development of extending knee joint contracture in rats. *Eur J Med Res*. 2024;29(1):298. doi:10.1186/s40001-024-01890-9
19. Monument MJ, Hart DA, Salo PT, Befus AD, Hildebrand KA. Posttraumatic elbow contractures: targeting neuroinflammatory fibrogenic mechanisms. *J Orthop Sci*. 2013;18(6):869–877. doi:10.1007/s00776-013-0447-5
20. Hildebrand KA, Sutherland C, Zhang M. Rabbit knee model of post-traumatic joint contractures: the long-term natural history of motion loss and myofibroblasts. *J Orthop Res*. 2004;22(2):313–320. doi:10.1016/j.orthres.2003.08.012
21. Hildebrand KA, Zhang M, Hart DA. Myofibroblast upregulators are elevated in joint capsules in posttraumatic contractures. *Clin Orthop Relat Res*. 2007;456:85–91. doi:10.1097/BLO.0b013e3180312c01
22. Doornberg JN, Bosse T, Cohen MS, et al. Temporary presence of myofibroblasts in human elbow capsule after trauma. *J Bone Joint Surg Am*. 2014;96(5):e36. doi:10.2106/JBJS.M.00388
23. Wang C, Dong J, Liu F, Liu N, Li L. 3D-printed PCL@BG scaffold integrated with SDF-1alpha-loaded hydrogel for enhancing local treatment of bone defects. *J Biol Eng*. 2024;18(1):1. doi:10.1186/s13036-023-00401-4
24. Li L, Tuan RS. Mechanism of traumatic heterotopic ossification: in search of injury-induced osteogenic factors. *J Cell Mol Med*. 2020;24(19):11046–11055. doi:10.1111/jcmm.15735
25. Li J, Sun Z, Luo G, et al. Quercetin attenuates trauma-induced heterotopic ossification by tuning immune cell infiltration and related inflammatory insult. *Front Immunol*. 2021;12:649285. doi:10.3389/fimmu.2021.649285
26. Xie J, Lin W, Huang L, et al. Bufalin suppresses the proliferation and metastasis of renal cell carcinoma by inhibiting the PI3K/Akt/mTOR signaling pathway. *Oncol Lett*. 2018;16(3):3867–3873. doi:10.3892/ol.2018.9111
27. Zhuang Z, Yu D, Chen Z, et al. Curcumin Inhibits Joint Contracture through PTEN demethylation and Targeting PI3K/Akt/mTOR pathway in myofibroblasts from human joint capsule. *Evid Based Complement Alternat Med*. 2019;2019:4301238. doi:10.1155/2019/4301238
28. Zhang Y, Lu S, Fan S, et al. Macrophage migration inhibitory factor activates the inflammatory response in joint capsule fibroblasts following post-traumatic joint contracture. *Aging (Albany NY)*. 2021;13(4):5804–5823. doi:10.18632/aging.202505
29. Zhang Y, Wang Z, Zong C, et al. Platelet-rich plasma attenuates the severity of joint capsule fibrosis following post-traumatic joint contracture in rats. *Front Bioeng Biotechnol*. 2022;10:1078527. doi:10.3389/fbioe.2022.1078527
30. Sasabe R, Sakamoto J, Goto K, et al. Effects of joint immobilization on changes in myofibroblasts and collagen in the rat knee contracture model. *J Orthop Res*. 2017;35(9):1998–2006. doi:10.1002/jor.23498
31. Sun Y, Li F, Fan C. Effect of pERK2 on extracellular matrix turnover of the fibrotic joint capsule in a post-traumatic joint contracture model. *Exp Ther Med*. 2016;11(2):547–552. doi:10.3892/etm.2015.2948
32. Zhang Y, Wu Z, Lu S, et al. Time-series expression profile analysis of post-traumatic joint contracture in rats at the early stages of the healing process. *J Inflamm Res*. 2023;16:1169–1181. doi:10.2147/JIR.S400557
33. Liu F, Dong J, Zhou D, Zhang Q. Identification of key candidate genes related to inflammatory osteolysis associated with vitamin E-Blended UHMWPE debris of orthopedic implants by integrated bioinformatics analysis and experimental confirmation. *J Inflamm Res*. 2021;14:3537–3554. doi:10.2147/JIR.S320839
34. Huang da W, Sherman BT, Lempicki RA. Bioinformatics enrichment tools: paths toward the comprehensive functional analysis of large gene lists. *Nucleic Acids Res*. 2009;37(1):1–13. doi:10.1093/nar/gkn923
35. Szklarczyk D, Gable AL, Lyon D, et al. STRING v11: protein-protein association networks with increased coverage, supporting functional discovery in genome-wide experimental datasets. *Nucleic Acids Res*. 2019;47(D1):D607–D613. doi:10.1093/nar/gky1131
36. Shannon P, Markiel A, Ozier O, et al. Cytoscape: a software environment for integrated models of biomolecular interaction networks. *Genome Res*. 2003;13(11):2498–2504. doi:10.1101/gr.1239303
37. Su G, Morris JH, Demchak B, Bader GD. Biological network exploration with Cytoscape 3. *Curr Protoc Bioinformatics*. 2014;47(813):11–24. doi:10.1002/0471250953.bi0813s47
38. Zhang Q, Lu S, Zhou D, Dong J, Liu F. PTGS2 identified as a biomarker of glucocorticoid-induced osteonecrosis of the femoral head and an enhancer of osteogenesis. *Genes Dis*. 2023;10(1):14–17. doi:10.1016/j.gendis.2022.01.005
39. Maere S, Heymans K, Kuiper M. BiNGO: a Cytoscape plugin to assess overrepresentation of gene ontology categories in biological networks. *Bioinformatics*. 2005;21(16):3448–3449. doi:10.1093/bioinformatics/bti551
40. Liu F, Dong J, Zhang P, Zhou D, Zhang Q. Transcriptome sequencing reveals key genes in three early phases of osteogenic, adipogenic, and chondrogenic differentiation of bone marrow mesenchymal stem cells in rats. *Front Mol Biosci*. 2021;8:782054. doi:10.3389/fmolb.2021.782054
41. Zhang Q, Dong J, Zhang P, Zhou D, Liu F. Dynamics of transcription factors in three early phases of osteogenic, adipogenic, and chondrogenic differentiation determining the fate of bone marrow mesenchymal stem cells in rats. *Front Cell Dev Biol*. 2021;9:768316. doi:10.3389/fcell.2021.768316

42. Kazezian Z, Bull AMJ. A review of the biomarkers and in vivo models for the diagnosis and treatment of heterotopic ossification following blast and trauma-induced injuries. *Bone*. 2021;143:115765. doi:10.1016/j.bone.2020.115765
43. Dunham CL, Castile RM, Chamberlain AM, Lake SP. The role of periarticular soft tissues in persistent motion loss in a rat model of posttraumatic elbow contracture. *J Bone Joint Surg Am*. 2019;101(5):e17. doi:10.2106/JBJS.18.00246
44. Dunham CL, Steenbock H, Brinckmann J, et al. Increased volume and collagen crosslinks drive soft tissue contribution to post-traumatic elbow contracture in an animal model. *J Orthop Res*. 2021;39(8):1800–1810. doi:10.1002/jor.24781
45. Dunham C, Havlioglu N, Chamberlain A, Lake S, Meyer G. Adipose stem cells exhibit mechanical memory and reduce fibrotic contracture in a rat elbow injury model. *FASEB J*. 2020;34(9):12976–12990. doi:10.1096/fj.202001274R
46. Milaras C, Lepetsos P, Dafou D, Potoupnis M, Tsiridis E. Association of Matrix Metalloproteinase (MMP) gene polymorphisms with knee osteoarthritis: a review of the literature. *Cureus*. 2021;13(10):e18607. doi:10.7759/cureus.18607
47. Cohen C, Leal MF, Loyola LC, et al. Genetic variants involved in extracellular matrix homeostasis play a role in the susceptibility to frozen shoulder: a case-control study. *J Orthop Res*. 2019;37(4):948–956. doi:10.1002/jor.24228
48. Rodrigues MP, et al. *MMP-1, MMP-8, and MMP-13 Gene Polymorphisms and Haplotype is a Risk Factor for Dupuytren Contracture: A Case-Control Study*. (N Y): Hand; 2024:15589447241242818. doi:10.1177/15589447241242818
49. Zhang R, Zhang R, Zhou T, et al. Preliminary investigation on the effect of extracorporeal shock wave combined with traction on joint contracture based on PTEN-PI3K/AKT pathway. *J Orthop Res*. 2024;42(2):339–348. doi:10.1002/jor.25687
50. Yan J, Feng G, Yang Y, et al. Nintedanib ameliorates osteoarthritis in mice by inhibiting synovial inflammation and fibrosis caused by M1 polarization of synovial macrophages via the MAPK / PI3K-AKT pathway. *FASEB J*. 2023;37(10):e23177. doi:10.1096/fj.202300944RR
51. Boudiffa M, Wade-Gueye NM, Guignandon A, et al. Bone sialoprotein deficiency impairs osteoclastogenesis and mineral resorption in vitro. *J Bone Miner Res*. 2010;25(12):2669–2679. doi:10.1002/jbmr.245
52. Ma Y, Chen B, Zhang B, et al. High expression of integrin-binding sialoprotein (IBSP) is associated with poor prognosis of osteosarcoma. *Aging (Albany NY)*. 2023;16(1):28–42. doi:10.18632/aging.205235
53. Hu L, Liu J, Xue H, et al. miRNA-92a-3p regulates osteoblast differentiation in patients with concomitant limb fractures and TBI via IBSP/PI3K-AKT inhibition. *Mol Ther Nucleic Acids*. 2021;23:1345–1359. doi:10.1016/j.omtn.2021.02.008
54. Chen Q, Shou P, Zhang L, et al. An osteopontin-integrin interaction plays a critical role in directing adipogenesis and osteogenesis by mesenchymal stem cells. *Stem Cells*. 2014;32(2):327–337. doi:10.1002/stem.1567
55. Si J, Wang C, Zhang D, Wang B, Zhou Y, Zhou Y. Osteopontin in Bone Metabolism and Bone Diseases. *Med Sci Monit*. 2020;26:e919159. doi:10.12659/MSM.919159
56. Lin Z, Tian XY, Huang XX, He LL, Xu F. microRNA-186 inhibition of PI3K-AKT pathway via SPP1 inhibits chondrocyte apoptosis in mice with osteoarthritis. *J Cell Physiol*. 2019;234(5):6042–6053. doi:10.1002/jcp.27225
57. Chen C, Liu J, Zhou F, et al. Next-generation sequencing of colorectal cancers in Chinese: identification of a recurrent frame-shift and gain-of-function indel mutation in the TFDPI Gene. *OMICS*. 2014;18(10):625–635. doi:10.1089/omi.2014.0058
58. Pellicelli M, Picard C, Wang D, Lavigne P, Moreau A. E2F1 and TFDPI Regulate PITX1 expression in normal and osteoarthritic articular chondrocytes. *PLoS One*. 2016;11(11):e0165951. doi:10.1371/journal.pone.0165951
59. Guo T, Han X, He J, et al. KDM6B interacts with TFDPI to activate P53 signaling in regulating mouse palatogenesis. *Elife*. 2022;11. doi:10.7554/eLife.74595
60. Zhao T, Su Z, Li Y, Zhang X, You Q. Chitinase-3 like-protein-1 function and its role in diseases. *Signal Transduct Target Ther*. 2020;5(1):201. doi:10.1038/s41392-020-00303-7
61. Endisha H, Rockel J, Jurisica I, Kapoor M. The complex landscape of microRNAs in articular cartilage: biology, pathology, and therapeutic targets. *JCI Insight*. 2018;3(17). doi:10.1172/jci.insight.121630
62. Li Q, Wu M, Fang G, et al. MicroRNA-186-5p downregulation inhibits osteoarthritis development by targeting MAPK1. *Mol Med Rep*. 2021;23(4). doi:10.3892/mmr.2021.11892
63. Liu N, Dong J, Li L, Liu F. Osteoimmune interactions and therapeutic potential of macrophage-derived small extracellular vesicles in bone-related diseases. *Int J Nanomed*. 2023;18:2163–2180. doi:10.2147/IJN.S403192
64. Liu N, Dong J, Li L, Zhou D, Liu F. The function and mechanism of anti-inflammatory factor metrn1 prevents the progression of inflammatory-mediated pathological bone osteolytic diseases. *J Inflamm Res*. 2024;17:1607–1619. doi:10.2147/JIR.S455790
65. Zhang Q, Sun W, Li T, Liu F. Polarization behavior of bone macrophage as well as associated osteoimmunity in glucocorticoid-induced osteonecrosis of the femoral Head. *J Inflamm Res*. 2023;16:879–894. doi:10.2147/JIR.S401968
66. Wang R, Bao H, Zhang S, et al. miR-186-5p promotes apoptosis by targeting IGF-1 in SH-SY5Y OGD/R model. *Int J Biol Sci*. 2018;14(13):1791–1799. doi:10.7150/ijbs.25352